UDC 551.509.314

OPTIMUM INFLUENCE RADII FOR INTERPOLATION WITH THE METHOD OF SUCCESSIVE CORRECTIONS[1]

J. J. STEPHENS and J. M. STITT[2]
Florida State University, Tallahassee, Fla.

ABSTRACT

A method of selecting optimum influence radii for the objective analysis of a scalar field using the method of successive corrections is presented for an arbitrary weight function. The Cressman weight function is used in a computational verification of the result.

A well-defined first pass optimum radius is found that increases with station separation, observational error, and wavelength of the true field for the average taken as the guess field.

1. INTRODUCTION

As introduced by Cressman (1959), the method of successive corrections interpolates observational discrepancies from a guess field at station locations to find estimates at points of a regular net. The interpolation is accomplished by a linear combination of the point discrepancies within some influence radius about the mesh point. The relative weight accorded each observation depends on its distance from the mesh point, as well as the number and distance of all other stations in the influence area through the normalization procedure. Several scans employing different influence radii are usually made in application with the choice of influence radius for a given scan based on a subjective judgment of the resulting analysis.

As shown by Gandin (1965) and Eddy (1967), the choice of weight function should depend on the field statistics. However, some success has been found with analytic functions that determine the form of the distance weighting. The influence radius must be specified.

A method of choosing influence radii in an optimum (least-squares sense) way for arbitrary scalar fields and weight functions is presented here for a simple statistical model of the data array. It is shown that the optimum radius for large signal-to-noise ratios is primarily dependent upon the average station separation. The variance spectra of the true and error fields are important for noisy observations. The results are illustrated with model fields of signal and error.

2. INTERPOLATION ERRORS

Estimates on the net are generated by a correction formula of the type

$$Z^e_{j,k}=Z^g_{j,k}+\sum_{m=1}^{M} w_n(r_m,R,M)\{Z^o(j\Delta x+r_m\cos\theta_m, k\Delta y+r_m\sin\theta_m)-Z^g(j\Delta x+r_m\cos\theta_m, k\Delta y+r_m\sin\theta_m)\} \quad (1)$$

where $Z^e_{j,k}$ denotes the grid point estimate at $(j\Delta k, k\Delta y)$ Z^o the irregularly distributed sample of the observed field, and Z^g the guess field. The weight function w_n is normalized to unity by

$$w_n(r_m,R,M)=\frac{W(r_m,R)}{\sum_{m=1}^{M} W(r_m,R)} \quad (2)$$

where M is the number of stations within the influence radius R. The unnormalized weight $W(r_m,R)$ is associated with the mth ordered station whose coordinates are r_m and θ_m in a local polar coordinate system with origin at $(j\Delta x, k\Delta y)$. It has been presumed that $x_0=y_0=0$ without loss of generality.

To some extent, the analysis depends on the character of the guess field. Here, it is assumed that the first scan begins with a guess field taken to be the average of the observed values. Further, if Z^T denotes the true field, the assumption $\overline{Z^o}=\overline{Z^T}$ is made. The observed field differs from the true field by

$$Z^o-Z^T=\epsilon \quad (3)$$

where ϵ is the observational error with zero mean. The grid point estimate is in error by

$$Z^e_{j,k}-Z^T_{j,k}=\delta_{j,k}. \quad (4)$$

If $Z'=Z^T-\overline{Z^T}$ and the station locations are identified by the subscript m, then the total error at a grid point after the first pass is

$$\delta_{j,k}=-Z'_{j,k}+\sum_{m=1}^{M} w_n(r_m,R,M)\{Z'_m+\epsilon_m\}. \quad (5)$$

With minimal restrictions, the true field deviation can be represented by

$$Z'(x,y)=\sum_{l=-\infty}^{\infty}\sum_{\kappa=-\infty}^{\infty} A_{l\kappa}e^{iK_x lx+iK_y\kappa y} \quad (6)$$

where $K_x=2\pi/L_x$ and $K_y=2\pi/L_y$ for interpolation in a

[1] Research supported by the National Severe Storms Laboratory, ESSA, under Grant E22-28-69(G) and U.S. Army Electronics Command, Contract No. DAAB07-69-C-0062 under Project THEMIS.

[2] Captain, U.S. Air Force. Completed while on A.F.I.T. (Air Force Institute of Technology) assignment at Florida State University.

rectangular domain of dimensions $L_x \times L_y$. Because of observational sampling limitations, a band-limited true field could be assumed. A similar representation is used for the error field:

$$\epsilon(x, y)=\sum_{l=-\infty}^{\infty}\sum_{\kappa=-\infty}^{\infty} E_{l\kappa}e^{iK_x lx+iK_y\kappa y}. \tag{7}$$

The discrepancy can then be written as

$$\delta_{j,k}=-Z'_{j,k}+\sum_{m=1}^{M} w_n(r_m, R, M)\left\{\sum_{l=-\infty}^{\infty}\sum_{\kappa=-\infty}^{\infty}(A_{l\kappa}+E_{l\kappa}) \times e^{iK_x lj\Delta x+iK_y\kappa k\Delta y}\times e^{iK_x lr_m\cos\theta_m+iK_y\kappa r_m\sin\theta_m}\right\}. \tag{8}$$

While equation (8) is a typical example, the relative station locations differ from point to point. This variability is removed here by assuming that the M station sites are randomly distributed within the influence area. Then r_m and θ_m are random variables with associated probability densities $p_m(r_m)$ and $f_m(\theta_m)$, respectively. The average of the weight for each station is then determined by averaging its location over all possible values. Since all stations in the domain may appear within the influence area for a particular realization of the data array, all must be considered. The total number of stations in the domain is denoted by N.

All values of θ_m in $(-\pi,\pi)$ are equally likely for a random data distribution. Since

$$\int_{-\infty}^{\infty} f_m(\theta_m)e^{iK_x lr_m\cos\theta_m+iK_y\kappa r_m\sin\theta_m}d\theta_m =\frac{1}{2\pi}\int_{-\pi}^{\pi} e^{iK_x lr_m\cos\theta_m+iK_y\kappa r_m\sin\theta_m}d\theta_m=J_0(r_mK_{l\kappa}) \tag{9}$$

where J_0 is the Bessel function of the first kind and order zero and

$$K_{l\kappa}=\sqrt{l^2K_x^2+\kappa^2K_y^2}, \tag{10}$$

the grid point estimate for average station location is

$$\delta_{j,k}=-Z'_{j,k}+\sum_{l=-\infty}^{\infty}\sum_{\kappa=-\infty}^{\infty} g_{l\kappa}(R, N, N)(A_{l\kappa}+E_{l\kappa}) \times e^{iK_x lj\Delta x+iK_y\kappa k\Delta y} \tag{11}$$

where

$$g_{l\kappa}(R, M, N)=\sum_{m=1}^{M} I_{l\kappa}(m, R, N) \tag{12}$$

and

$$I_{l\kappa}(m, R, N)=\int_0^{\infty} p_m(r_m)w_n(r_m, R, N)J_0(r_mK_{l\kappa})dr_m. \tag{13}$$

As implied by their dependence on N, the relative weights $w_n(r_m,R,N)$ as well as $I_{l\kappa}$ (m,R,N) and $g_{l\kappa}(R,M,N)$ are taken to be functions of all the average distances from the mesh point to the stations.

The averaging above essentially determines the average weight for each of the ordered stations. It does not properly account for the probability that a station may not be within the influence area. For instance, there is a finite probability $P_N\{r_N<R\}$ that the most distant station is within the influence radius. Consequently, the discrepancy is taken to be

$$\delta_{j,k}=(1-P_N)\delta_{j,k}(N-1)+P_NF_{j,k}^{(N)} \tag{14}$$

where the notation

$$F_{j,k}^{(L)}=-Z'_{j,k}+\sum_{l=-\infty}^{\infty}\sum_{\kappa=-\infty}^{\infty} g_{l\kappa}(R,L,N)(A_{l\kappa}+E_{l\kappa})e^{iK_x lj\Delta x+iK_y\kappa k\Delta y} \tag{15}$$

has been introduced. Here, $\delta_{j,k}$ $(N-1)$ is the discrepancy to be expected when the Nth station is not in the influence area in a probabilistic sense. Similar considerations for the $(N-1)$th station lead to

$$\delta_{j,k}(N-1)=(1-P_{N-1})\delta_{j,k}(N-2)+P_{N-1}F_{j,k}^{(N-1)}. \tag{16}$$

After all the ordered stations are considered sequentially, the discrepancy for the closest station is

$$\delta_{j,k}(1)=(1-P_1)\{-Z'_{j,k}\}+P_1F_{j,k}^{(1)} \tag{17}$$

since the discrepancy is $-Z'_{j,k}$ if the first station is outside of R. These can be combined to write

$$\delta_{j,k}=-Z'_{j,k}+\sum_{l=-\infty}^{\infty}\sum_{\kappa=-\infty}^{\infty} G_{l\kappa}(A_{l\kappa}+E_{l\kappa})e^{iK_x lj\Delta x+iK_y\kappa k\Delta y} \tag{18}$$

where

$$G_{l\kappa}=\sum_{m=1}^{N} H_mI_{l\kappa}(m, R, N), \tag{19}$$

$H_N=P_N$, and

$$H_m=P_m+\sum_{j=m+1}^{N} P_j\prod_{k=m}^{j-1}(1-P_k);\ m<N. \tag{20}$$

The form of the probability weighting H_m obtained by direct substitution is

$$H_m=P_N+\sum_{j=m}^{N-1} P_j\prod_{l=j+1}^{N}(1-P_l). \tag{21}$$

Since $H_m\sim P_m$, the form suggested by (20) is preferred. In the examples shown below, stations are included if $P_m\geq 0.005$.

Clearly, the distance to the mth ordered station depends on the location of the $(m-1)$th station. Hence, $p_m(r_m)$ should be a joint probability density. However, the essential behavior of the discrepancy is retained by treating the $p_m(r_m)$ as independent distributions. Their behavior is discussed further below.

The domain of interpolation is divided as $L_x=J\Delta x$ and $L_y=K\Delta y$ to form the mesh. The variance of the interpolation error is

$$\sigma^2=\frac{1}{JK}\sum_{j=0}^{J-1}\sum_{k=0}^{K-1}|\delta_{j,k}|^2, \tag{22}$$

or

$$\sigma^2=\sum_{l=-\infty}^{\infty}\sum_{\kappa=-\infty}^{\infty}\{|A_{l\kappa}|^2(1-G_{l\kappa})^2+(A_{l\kappa}E_{l\kappa}^*+E_{l\kappa}A_{l\kappa}^*) \times(G_{l\kappa}^2-G_{l\kappa})+|E_{l\kappa}|^2G_{l\kappa}^2\} \tag{23}$$

when (18) is incorporated. If it is assumed that the error component is uncorrelated with any other field, then the grid point error variance for the first pass reduces to

$$\sigma^2_{(1)}=\sum_{l=-\infty}^{\infty}\sum_{\kappa=-\infty}^{\infty}(|A_{l\kappa}|^2(1-G_{l\kappa})^2+|E_{l\kappa}|^2G^2_{l\kappa}). \quad (24)$$

Before considering particular examples of (24), it will be useful to develop an interpolation error relation when a nontrivial guess field is provided. In particular, the guess field taken is that whose grid point discrepancy $\delta^{(1)}_{j,k}$ is given by (18). On the second pass, the interpolation error is

$$\delta^{(2)}_{j,k}=\delta^{(1)}_{j,k}+\sum_{m=1}^{N}w_n(r_m, R_2, N)\{\epsilon_m-\delta^{(1)}_m\} \quad (25)$$

where R_2 is the second pass influence radius. In practice, the deviation at a station is given by a linear combination of the four surrounding grid points. In this analysis, the corresponding station discrepancy is found by taking the centroid of the mesh area as the station location. If equation (18) is written as

$$\delta^{(1)}_{(x,y)}=\sum_{l=-\infty}^{\infty}\sum_{\kappa=-\infty}^{\infty}H_{l\kappa}e^{iK_xlx+iK_y\kappa y} \quad (26)$$

where

$$H_{l\kappa}=(A_{l\kappa}+E_{l\kappa})G_{l\kappa}-A_{l\kappa}, \quad (27)$$

then (26) evaluated at the surrounding mesh points and averaged leads to

$$\delta^{(1)}_m=\tfrac{1}{4}\sum_{l=-\infty}^{\infty}\sum_{\kappa=-\infty}^{\infty}H_{l\kappa}e^{iK_xlj\Delta x+iK_y\kappa k\Delta y}e^{iK_xlr_m\cos\theta_m+iK_y\kappa r_m\sin\theta_m}\times\left(2\cos\left(K_xl\frac{\Delta x}{2}-K_y\kappa\frac{\Delta y}{2}\right)+2\cos\left(K_xl\frac{\Delta x}{2}+K_y\kappa\frac{\Delta y}{2}\right)\right). \quad (28)$$

The observational error is treated as in the first pass. After averaging the station locations and accounting for the sampling discreteness, the expected value of the second pass discrepancy is

$$\delta^{(2)}_{j,k}=\sum_{l=-\infty}^{\infty}\sum_{\kappa=-\infty}^{\infty}\left\{H^{(1)}_{l\kappa}+G^{(2)}_{l\kappa}\times\left(E_{l\kappa}-H^{(1)}_{l\kappa}\cos\left(K_xl\frac{\Delta x}{2}\right)\cos\left(K_y\kappa\frac{\Delta y}{2}\right)\right)\right\}e^{iK_xlj\Delta x+iK_y\kappa k\Delta y} \quad (29)$$

where $G^{(2)}_{l\kappa}$ differs from $G_{l\kappa}$ only in that the latter is evaluated for the optimum influence radius for the first pass.

The discrepancy variance for uncorrelated observational error is

$$\sigma^2_{(2)}=\sum_{l=-\infty}^{\infty}\sum_{\kappa=-\infty}^{\infty}\left\{|A_{l\kappa}|^2(1-G_{l\kappa})^2\left(1-G^{(2)}_{l\kappa}\cos\left(K_xl\frac{\Delta x}{2}\right)\times\cos\left(K_y\kappa\frac{\Delta y}{2}\right)\right)^2+|E_{l\kappa}|^2\left[G_{l\kappa}\left(1-G^{(2)}_{l\kappa}\cos\left(K_xl\frac{\Delta x}{2}\right)\times\cos\left(K_x\kappa\frac{\Delta y}{2}\right)\right)+G^{(2)}_{l\kappa}\right]^2\right\}. \quad (30)$$

Equations (24) and (30) constitute models of the error variances to be expected on the first and second passes principally in that the error field is presumed to be uncorrelated and the distribution of observing sites is random. The variances suggested by (24) and (30) will be compared to more realistic examples after specifiying details of the error field and determining the distance probability distribution.

3. DISTANCE DISTRIBUTIONS

Empirical probability densities for the spacing of randomly distributed stations away from a grid point are used here. For discussing them, it is convenient to introduce several parameters.

The average station density, $\bar{\eta}$, is defined by the ratio

$$\bar{\eta}=\frac{N}{A} \quad (31)$$

where N is the total number of stations in the area A. An operational definition of the average station separation, d, is determined by regarding A in terms of an equivalent rectangular area divided into N equal, square cells. It follows that $\bar{\eta}=1/d^2$.

Another important length scale is obtained by considering the number of stations $I(\rho)$ within a radius ρ about an arbitrary point in the field:

$$I(\rho)=\int_0^{2\pi}\int_0^{\rho}\bar{\eta}\,r\,dr\,d\theta=\frac{\pi\rho^2}{d^2}. \quad (32)$$

If attention is restricted to integers $I(\rho_m)=m$, then

$$\rho_m=\sqrt{\frac{m}{\pi}}\,d. \quad (33)$$

Here, ρ_m is the average distance to the mth ordered station.

Empirical distributions were determined by generating station locations in the plane with a pseudorandom number generator. Five such realizations were found for each of several station densities. A 21 × 21 point grid was placed in the region for each realization. The distances to the closest 10 stations were stratified according to radius interval for each grid point. The average distribution for all grid points and realizations is well represented by the Pearson type III probability density (Zelen and Severo 1964) in the form

$$p_m(r_m)=\frac{(r_m/\Delta x)^{\alpha-1}\exp\{-r_m/\beta\rho_m\}}{\beta^\alpha\Gamma(\alpha)(\rho_m/\Delta x)^\alpha} \quad (34)$$

provided the distribution parameters α and β satisfy

$$\alpha\beta=1-\frac{1}{3m^{3/2}(d/\Delta x)} \quad (35)$$

and

$$\beta^2\alpha=\frac{(d/\Delta x)}{14m^{9/8}}. \quad (36)$$

Here, $\Gamma(\alpha)$ is the gamma function. The arbitrary forms in (35) and (36) as well as the numerical factors and ex-

ponents were chosen to match the observed mean and variance. The behavior with d is as suggested by observation. All distances are expressed in units of Δx.

4. COMPUTATIONAL ILLUSTRATIONS

The weight function chosen to illustrate the formulation is that due to Cressman (1959):

$$W(r,R)=\frac{R^2-r^2}{R^2+r^2}. \tag{37}$$

The distance influence functions were evaluated with 20-point Gaussian quadrature. As indicated by integrals of the probability density, better than three significant figure accuracy was obtained for the results reported here, except as noted.

As an initial test of the theory, 20 random station arrays with $d = 2.8\ \Delta x$ were generated, and the analytic field

$$Z'(x, y)=A \sin\left(\frac{2\pi x}{20\Delta x}\right) \cos\left(\frac{2\pi y}{80\Delta y}\right) \tag{38}$$

was evaluated at each station location. Errors drawn from a normal distribution with a variance 1/250 of the field variance were then added to the "observations." These were treated as band-limited white noise in the model. Interpolated values of a 21×21 point net were found for each of the 20 realizations using the method of successive corrections. The average and envelope of the interpolation results are shown in figure 1. The optimum influence radius for the experimental average occurs at $R/d\sim1.6$ for this field. Smaller values are indicated for the maximum and theory. In general, the theoretical results given by equation (24) presume a better utilization of data for small R than might be obtained for an "average" array under the least-squares criterion. As shown below, however, the results for a particular station array may differ markedly. Although the interpolation error at the optimum radius may differ significantly with each array realization, the choice $R\sim1.6d$ leads to negligible difference in the error for a given array and for this field. Both the observational average and theory suggest that the influence radius should be overestimated, rather than underestimated.

The average of 20 station array realizations represents a homogeneous data distribution. In such a case, there is excellent agreement between theory and observation for large R. The observed optimum radius varies with the particular realization; it may be larger or smaller than the theory predicts.

The grid and station array shown in figure 2 was used to illustrate typical results for an essentially homogeneous data array. In addition to equation (38), the field

$$Z'(x,y)=A \sin\left(\frac{2\pi x}{60\Delta x}\right) \tag{39}$$

was evaluated at the stations. In this case, no errors were added so that the discrepancies are due to interpolation

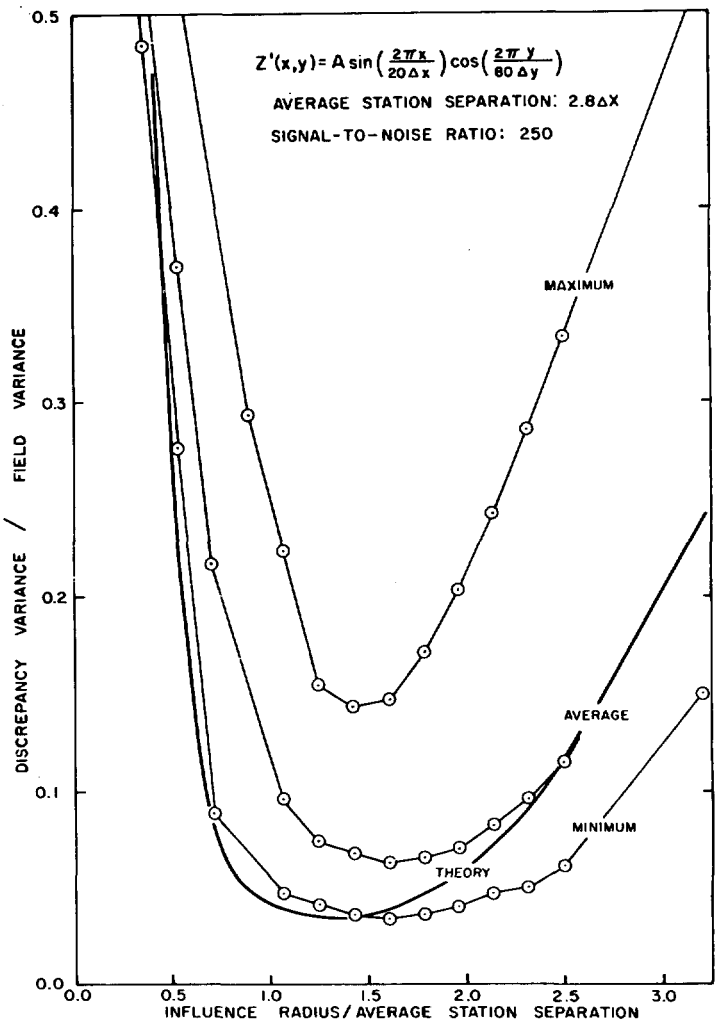

FIGURE 1.—Theoretical and experimental normalized interpolation discrepancy variances for an ensemble of randomly distributed station arrays.

error alone. Comparisons of the actual and predicted grid point discrepancies after two passes are shown in figures 3 and 4. Again, the predicted results are obtained from equations (24) and (30). While the actual first pass interpolation shown in figure 3 is more accurate than the theory suggests, there is excellent correspondence between the optimum radii. As before, the large-radius agreement for homogeneous data distributions might be noted. In view of the logarithmic scale, the second pass discrepancies are in substantial agreement. It was found experimentally that the optimum influence radius for the second pass was less than that for the first pass, provided that the average was used for the first pass guess field and that the second pass begins with the optimum first pass results. Theory suggests a smaller error and a less well-defined optimum radius for the second pass.

The results shown in figure 4 for a wavelength of 60 Δx once again show a smaller first pass experimental error. A larger influence radius is indicated for the model. The second pass theory is again too optimistic.

The same fields were evaluated for the array shown in figure 5. The station distribution is a realistic one in that

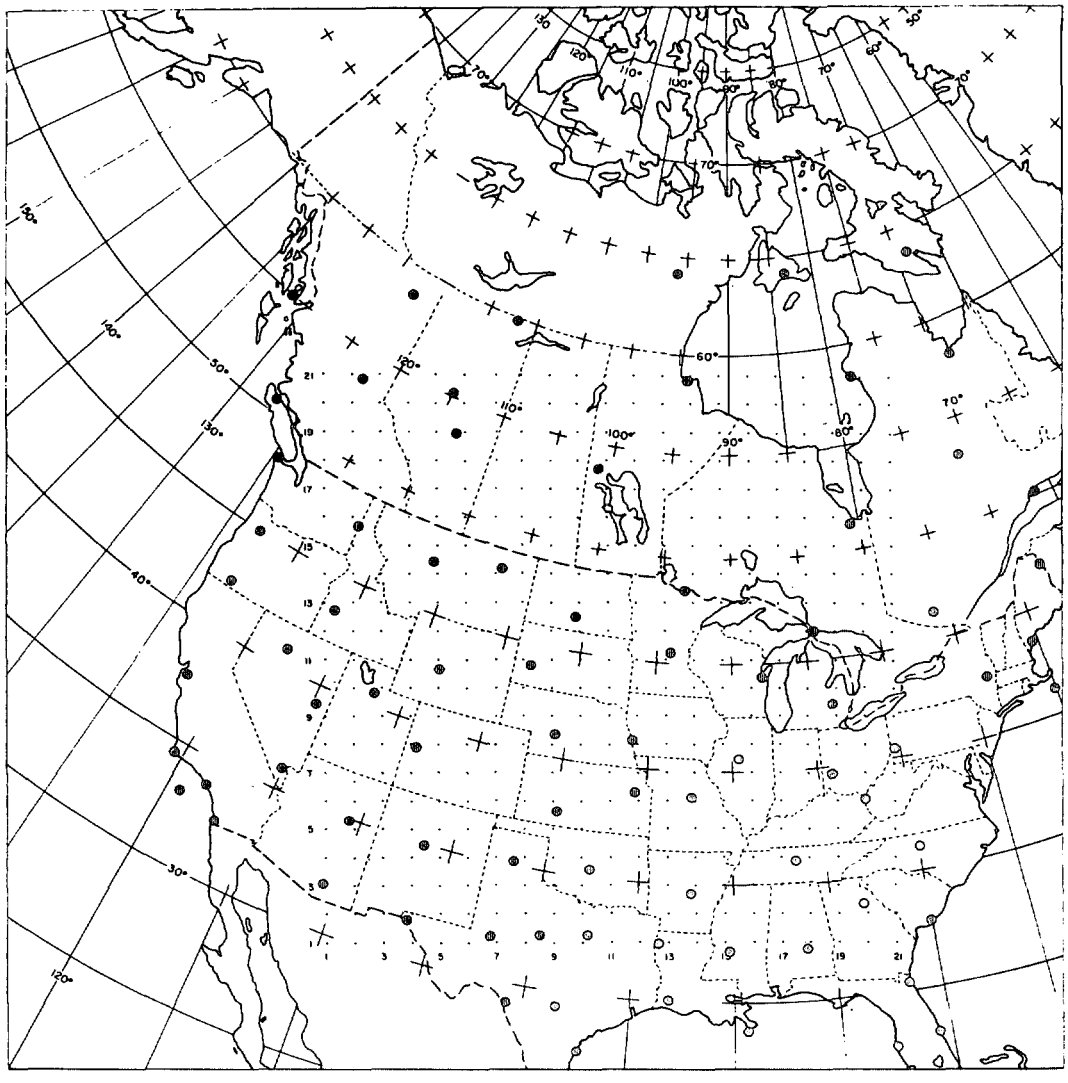

FIGURE 2.—Grid and station array for an essentially homogeneous data distribution.

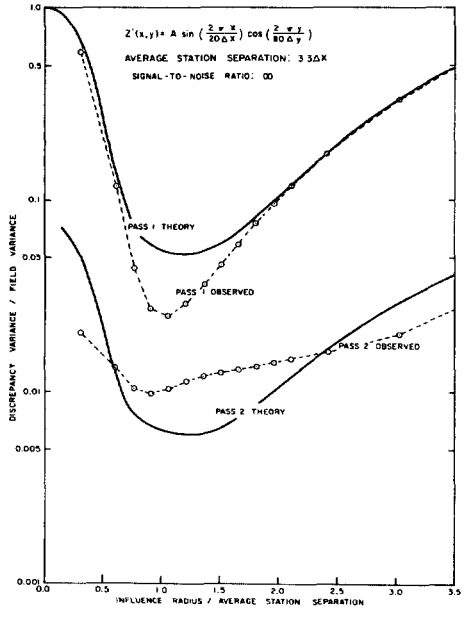

FIGURE 3.—Theoretical and experimental normalized discrepancy variances for a homogeneous data distribution. A two-dimensional true field and an average station separation of 3.3 Δx have been used.

a data void exists beyond the oceanic boundary. The largest of the errors summarized in figures 6 and 7 are in the data void. This leads to a greater discrepancy variance and a larger influence radius than result from a more homogeneous array.

The existence of a well-defined first pass optimum influence radius depends primarily on the balance of the decrease due to the inclusion of additional stations and the increase in interpolation error with increasing distance. While most applications of successive corrections would be to fields with large signal-to-noise ratios, it is of interest to note the variation with a substantial increase in the noise level. As shown in figure 8, as the observational error variance is increased to match the field variance, the discrepancy increases, as does the optimum influence radius. For a noisy field, the contribution of the error of observation decreases with increasing influence radius as more samples are included. The presence of additive, random noise does not significantly affect the results for a wavelength of 20 Δx and a sampling interval of 2.8 Δx.

As expected, the optimum influence radius increases with station separation, along with the corresponding

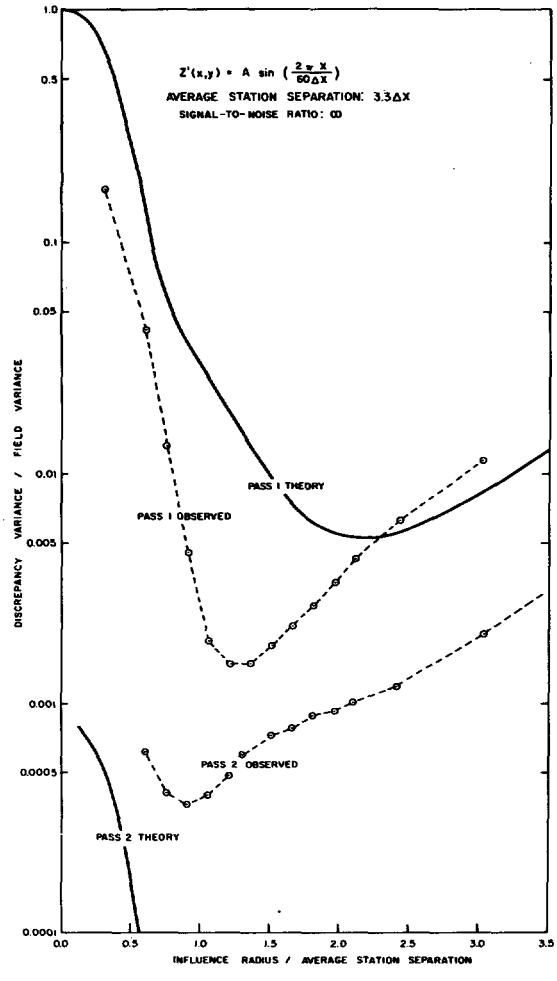

FIGURE 4.—Theoretical and experimental normalized discrepancy variances for a homogeneous data distribution. A one-dimensional true field and an average station separation of 3.3 Δx have been used.

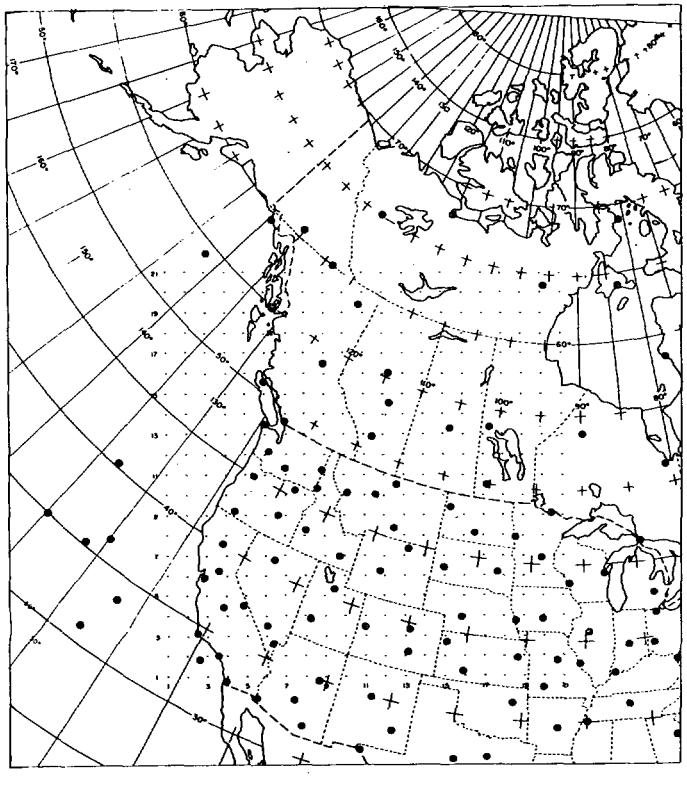

FIGURE 5.—Grid and station array for a biased data distribution.

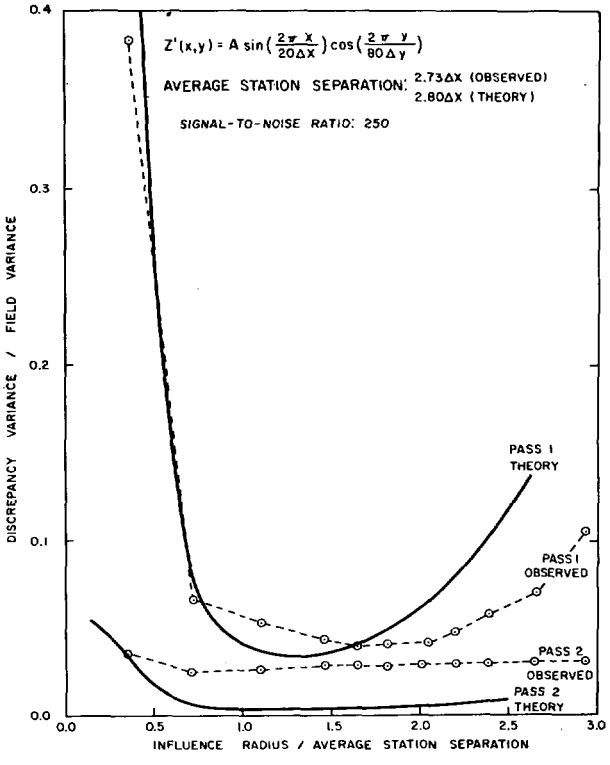

FIGURE 6.—Theoretical and experimental normalized discrepancy variances for a biased data distribution. A two-dimensional field with error has been used.

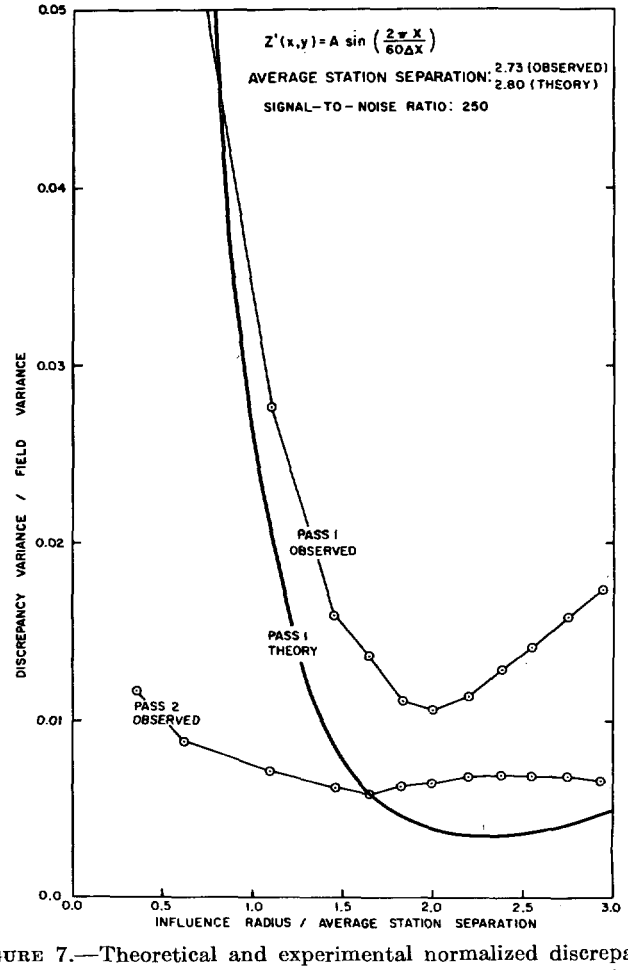

FIGURE 7.—Theoretical and experimental normalized discrepancy variances for a biased data distribution. A one-dimensional field with error has been used.

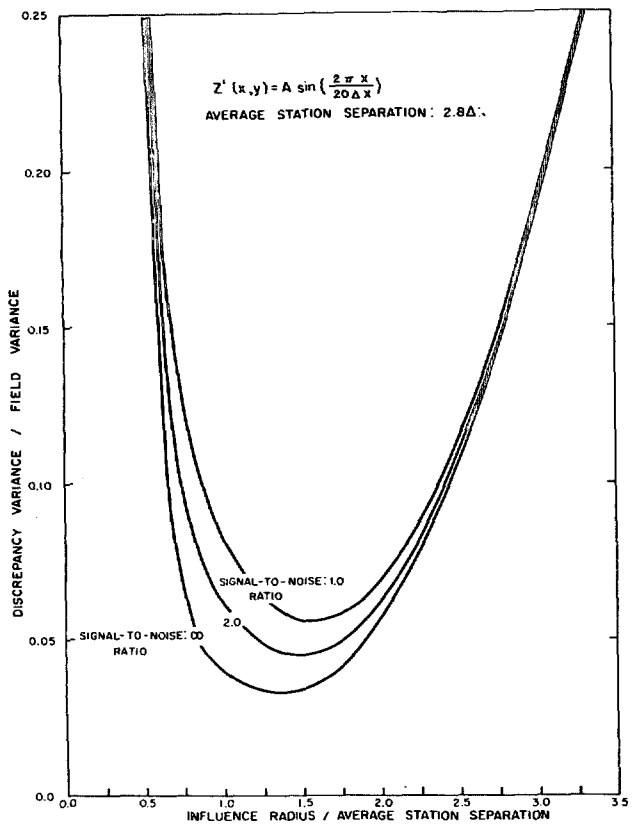

FIGURE 8.—Theoretical normalized discrepancy variance for three noise levels. A one-dimensional field with an average station separation of 2.8 Δx has been used.

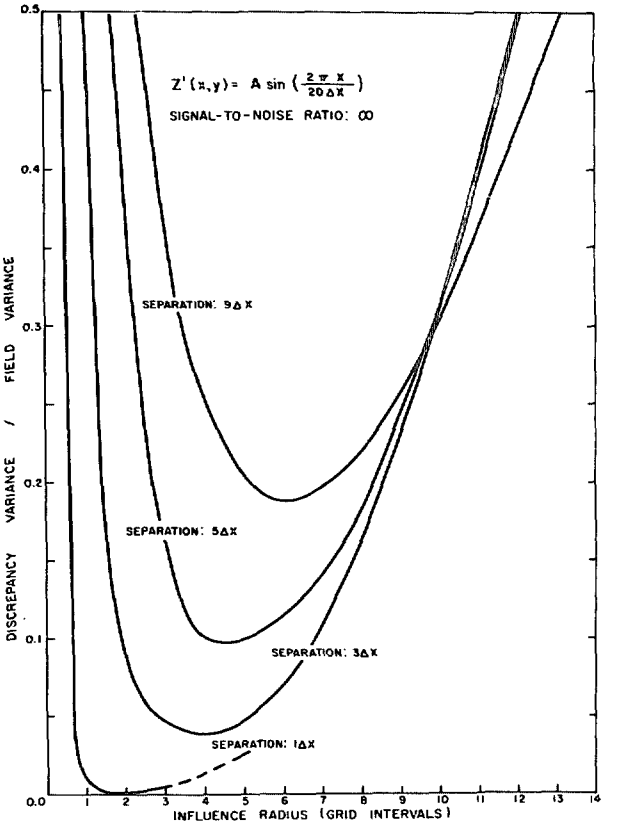

FIGURE 9.—Theoretical normalized discrepancy variance for four station separations. A one-dimensional true field with an average station separation of 2.8 Δx has been used.

interpolation error. This is shown in figure 9. The large-radius results indicate that as the influence radius exceeds one-half wavelength the error is greater for smaller separations. However, this periodic behavior was not explored further. As suggested by the dashed results for $d=1\ \Delta x$, the computations are not sufficiently accurate for large R/d.

The variation with wavelength is illustrated in figure 10 for a separation $d=2.8\ \Delta x$. Computations for wavelengths less than 20 Δx suggest that the limiting optimum radius for the shortest definable wave is the average distance to the closest station. Within the computational accuracy, the long-wave limit appears to be an optimum radius of twice the average station separation. Thus, if the signal-to-noise ratio is large, the effective range of optimum radii satisfies the approximate inequality $1<R/d<2$. Although any field is permitted with the theoretical model, a satisfactory optimum radius can be obtained from figure 10 with an approximate knowledge of the field spectrum and a suitably adjusted station density. If κ_j is the relative contribution of the jth spectral component and $e_j(R)$ the corresponding interpolation error, the optimum R is determined by minimizing the quantity

$$E(R)=\sum_j \kappa_j e_j(R) \qquad (40)$$

with respect to R.

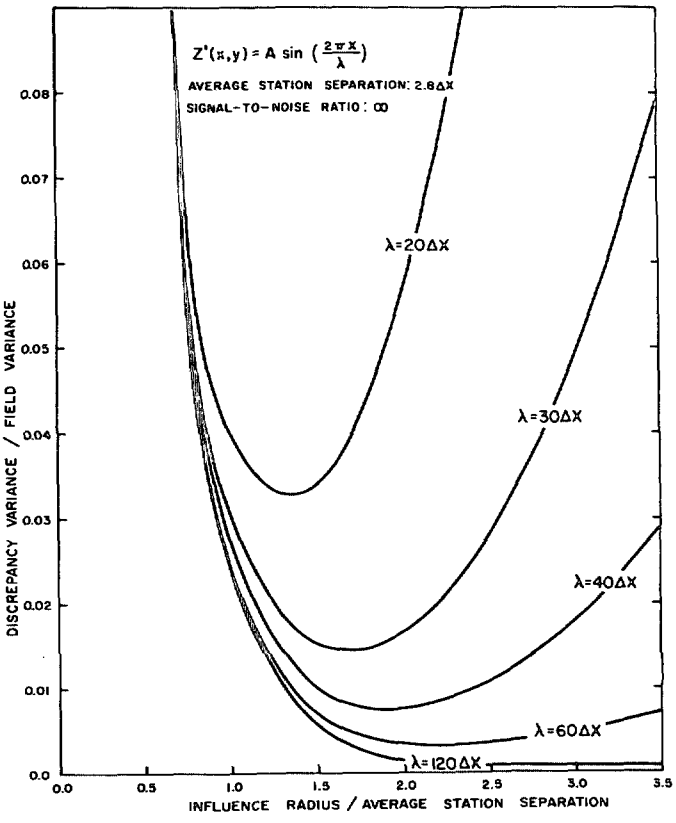

FIGURE 10.—Theoretical normalized discrepancy variance for five one-dimensional waves. An average station separation of 2.8 Δx has been used with no error.

5. CONCLUSIONS

Although variations are found for different arrays, there is substantial agreement between the experimental and model discrepancy variances presented here. As expected, the optimum influence radius increases with data separation and observational error. First pass results for one-dimensional monochromatic fields with the average used as a guess field suggest that $1<R/d<2$. Because a particular guess field was used, the second pass has not been explored extensively. Although the optimum for the second pass is not as well defined as that for the first, experiment suggests a smaller value.

If the average is used as a guess field, an optimum first pass radius can be estimated. Otherwise, the model can accommodate arbitrary guess and true fields in the presence of random noise. The theory for an arbitrary guess field would proceed from the formulation for the second pass used here.

In addition to the determination of optimum influence radii for the method of successive corrections, the analysis technique employed here can be used to determine the properties of other arithmetic operations applied to data distributed randomly in two dimensions.

ACKNOWLEDGMENTS

The author is indebted to Mr. O. Talagrand of the Geophysical Fluid Dynamics Laboratory, ESSA, for his constructive and complete review and to Mrs. Janina Richards for her care in typing the manuscript.

REFERENCES

Cressman, George P., "An Operational Objective Analysis System," *Monthly Weather Review*, Vol. 87, No. 10, Oct. **1959**, pp. 367–374.

Eddy, Amos, "The Statistical Objective Analysis of Scalar Data Fields," *Journal of Applied Meteorology*, Vol. 6, No. 4, Aug. **1967**, pp. 597–609.

Gandin, L. S., *Objective Analysis of Meteorological Fields* (*Ob''ektivnyi analiz meteorologicheskikh polei*, 1963), Israel Program for Scientific Translations, Jerusalem, **1965**, 242 pp.

Zelen, M., and Severo, N. C., "Probability Functions," *Applied Mathematics Series* 55, National Bureau of Standards, Washington, D.C., **1964**, 1,046 pp. (see pp. 925–995).

[*Received November 20, 1969; revised March 27, 1970*]